Empirically-Derived Corrections for Facility Effects in Performance and Plume Measurements of Hall Thrusters

Bryan M. Reid, Ph.D.[1]
The University of Michigan, Ann Arbor, MI, 48109, USA

Abstract: **Performance measurements were taken with the H6 hall thruster at facility pressures ranging from 1.3 to 2.0×10^{-5} torr. The facility pressure was changed by injecting xenon gas rather than discrete changes in pumping speed. Measurements of thrust, discharge current, and far-field current density were taken at each pressure and later corrected to remove the impact of facility effects using linear extrapolation of the measurements. Results at 6 kW and 8 kW indicate that thruster efficiency was augmented by as much as 3% due to facility effects. Corrected current density profiles reduced integrated current by >10% and reduced beam divergence half angle by 20 degrees. Separate analytical corrections to the discharge current and thrust that used entrainment area required a hemisphere at the thruster outer diameter to account for the measured variation with pressure. The corrections indicate that 50-60% of ionized facility neutrals do not contribute to thrust; suggesting that many of these ions may have large divergence angles and contribute directly to the increased wings that are measured at higher facility pressure. These analytical and experimental results were leveraged to recommended facility pressure limitations that minimize facility effects for future measurements.**

Nomenclature

A_{en}	=	entrainment area for facility neutrals
I_{corr}	=	corrected discharge current
I_D	=	measured discharge current
I_{en}	=	beam current due to entrained neutrals
k_B	=	Boltzmann's constant
$\dot{m}_a$	=	anode mass flow rate
$\dot{m}_{en}$	=	entrained mass flow rate
m_{xe}	=	xenon atom mass
n_n	=	neutral number density
P	=	facility pressure
T	=	temperature of facility neutrals
τ	=	thrust
τ_{corr}	=	corrected thrust
ζ_{en}	=	entrainment utilization efficiency

---

[1] Currently Technical Staff, Advanced Capabilities and Technologies Group, MIT Lincoln Laboratory, b.reid@ll.mit.edu

I.   Introduction

Understanding hall thruster on-orbit performance is critical to their continued adoption for near-earth and interplanetary missions. There have been numerous investigations and methods proposed to correct laboratory measurements to account for finite facility pressure.[1-8] Several authors have noted the linear relationship of current density with pressure and have extrapolated results to vacuum pressure. This paper leverages those works and extends the principle to thrust and discharge current to investigate the role that facility pressure plays in overall thruster performance.

Recent work suggested that cathode placement and magnetic field configuration contributed to enhanced electron mobility and that entrainment area is not the primary factor when considering facility effects.[8] Although these recent results are worth pursuing, this paper continues with the existing principle that facility neutrals are entrained and augment thruster performance via internal and near-field ionization and acceleration.

II.   Experimental Description

A. Vacuum facility

Experiments were performed in the Large Vacuum Test Facility (LVTF) at the University of Michigan's Plasmadynamics and Electric Propulsion Laboratory (PEPL). The LVTF is a 6-m-diameter, 9-m-long, cylindrical, stainless steel vacuum chamber. The chamber operates with seven cryopumps and LN2 shrouds that produce a nominal pumping speed of 240,000 l/s of xenon. The LVTF is described in greater detail in elsewhere.[6, 9]

B. Hall thruster

Experiments were performed using a 6-kW laboratory model Hall thruster[10-14] that has a demonstrated throttling range of approximately 1-10 kW, 100-600 mN, and 1000-3000 s specific impulse. The thruster was constructed with 8 individual outer coils, a single inner coil, and an internal trim coil. The trim coil was not used for the data presented in this paper. The thruster was equipped with a center-mounted LaB6 hollow cathode that was operated at 7% of the anode mass flow rate. The thruster was positioned so that it was elevated to chamber centerline, allowing the plume to expand for approximately 4-7 m along the chamber axis depending on the experiment.

C. Thrust Stand

Tests were performed with a NASA GRC-type inverted pendulum thrust stand. The control electronics were replaced with a commercial PID controller and linear amplifier, allowing operation with a single control coil. The thrust stand is described in greater detail in Ref 15.

D. Faraday probe

The Faraday probe used in these measurements was the JPL nude probe.[16] The collector is a 23.1-mm aluminum disk that was tungsten coated to reduce secondary electron emission due to high-energy impacting ions. The collector and guard ring were biased at -15 V with respect to ground and the current collected at the probe was measured across a 107.1 Ω current shunt. The probe was located at 104.5 ± 0.5 cm downstream of the thruster exit plane, with the axis of rotation located on thruster centerline at the exit plane.

III.   Results

A. Faraday Probe Measurements
1. Variation with anode flow rate

Results for the far-field Faraday probe measurements are shown in Figure 1 for thruster operation at 300 V and 5, 10, 20, and 30 mg/s. Measurements were taken on a 1-m circle that extended from ± 180º from thruster centerline. The data were highly symmetric about thruster centerline and indicated a consistent increase in the current density measured in the wings of the profile ($|\theta| > 90º$). This increase in current density confirmed the linear dependence of CEX collisions on facility pressure that was observed and predicted in previous work.[16, 17] These data also showed a distinct "double peak" at thruster centerline that was produced by the annular discharge channel. The "double peak" was significantly more apparent at lower flow rates; consistent with the expectation that there were more CEX collisions and hence, more beam spreading at higher flow rates due to the elevated facility pressure. It is worth noting that the characteristic bump in the wings is no longer prominent at 5 mg/s profile (noticeable at approximately 60° for 10-30 mg/s).

Azziz[2] attempted to correct for current density in the wings by subtracting the measured current density at 90 degrees, without success. However, these data indicate that there is a measureable current density at 180 degrees from the thruster exit, which would further reduce the impact of the subtraction method.
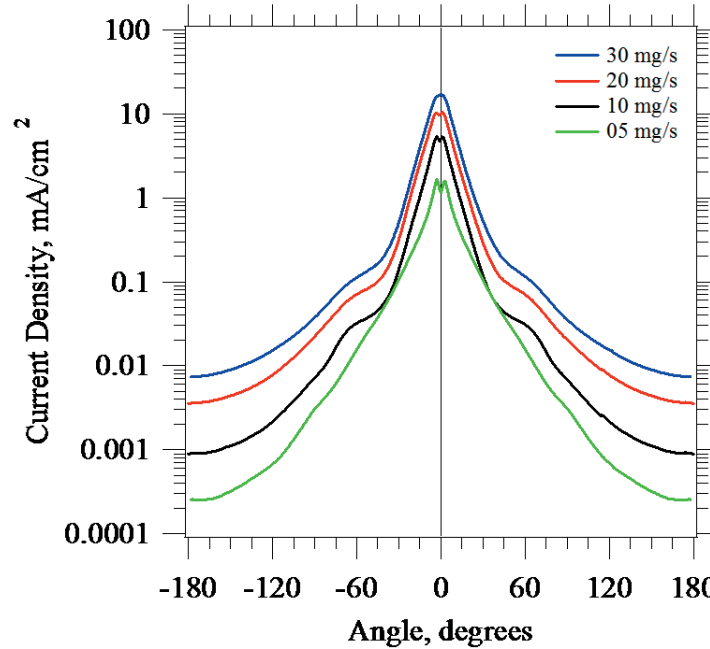

**Figure 1. Comparison of current density profiles for operation
at 300 V and 5, 10, 20, and 30 mg/s.**

Current density traces were processed to extract the integrated beam current and 95% half angle using methods in the literature.[4] The divergence was calculated independently for the left and right portion of the profile, typically varying by less than one degree. The average result is shown in the table with the measured discharge current and integrated ion beam current. The integrated current was approximately 5% higher than the measured discharge current for all operating conditions.

Table 1. Measured and calculated quantities for thruster operation at 300V and 5, 10, 20, and 30 mg/s.

Anode Flow Rate (mg/s)	Measured Discharge Current (A)	Integrated Beam Current (A)	Current Ratio	95% half Angle (deg)
5	3.95	4.17	1.05	62
10	8.70	9.29	1.07	63
20	20.0	21.2	1.06	65
30	33.5	34.3	1.02	66

2. Variation with facility pressure

Pressure was varied by injecting xenon gas at the center of the chamber at 50, 75, 100, 125 and 150 sccm. The injection port was located beneath supporting equipment and directed away from the thruster to increase uniformity and minimize direct ingestion into the thruster.

Far-field faraday probe measurements were recorded with the thruster operating at 300 V and 20 mg/s and facility pressures ranging from 1.3 to 2.0×10^{-5} torr-xe, corresponding to the injected xenon levels. These measurements are shown in Figure 2 and exhibit a clear trend of increased current density in the wings. The central portion of the plume remained mainly unaffected as pressure was changed. A similar set of measurements were performed by showing the same trend of increased current density in the wings with increased facility pressure.[4] The vacuum-extrapolated current density profile is also shown in Figure 2, discussed further in following sections.
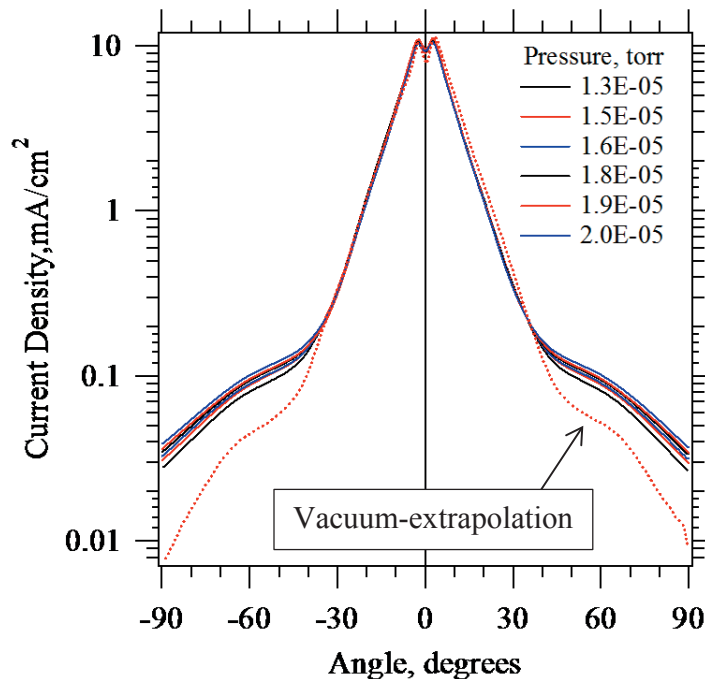
**Figure 2. Comparison of current density profiles for 300 V and
20 mg/s thruster operation, for all facility pressures.**

3. Vacuum extrapolation

The increase in current density in the wings followed a distinct linear trend with facility pressure that is shown in Figure 3 for locations from 50 to 90º. This relationship allowed the current density to be extrapolated to zero facility pressure, offering an approximation of the true vacuum current density distribution. The linear relationship shown in Figure 3 persisted at all locations throughout the plume; however, the relationship was less distinct at angles below ± 30º.

The vacuum extrapolation method was insensitive to a precise measurement of facility pressure. This was an important characteristic since most facilities employ typical Bayard-Alpert ion gauges, which have absolute pressure uncertainties of at least ± 20%. During analysis, changes of ± 50% in the pressure reading (for all pressures) resulted in an imperceptible change in the extrapolated current density shape, total current, and plume divergence. However, the same features were heavily dependent on the slope of the pressure reading, which was dependent on the gauge type and accuracy of the linear fit. In this study, two independent pressure readings were recorded and averaged to obtain the reported facility pressure.

 Current density traces were processed using the same method as before. Results of the measured and vacuum-extrapolated current density profiles are shown in Table 2. The 95% half angle increases linearly with pressure as expected from visual comparison of the current density profiles in Figure 4. The integrated current also increases with pressure, however the 2.0×10^{-5} torr data point departs from this trend. Closer examination of the current trace shows a deficit in the peak current density, but this deficit in not explained from the raw experimental data.
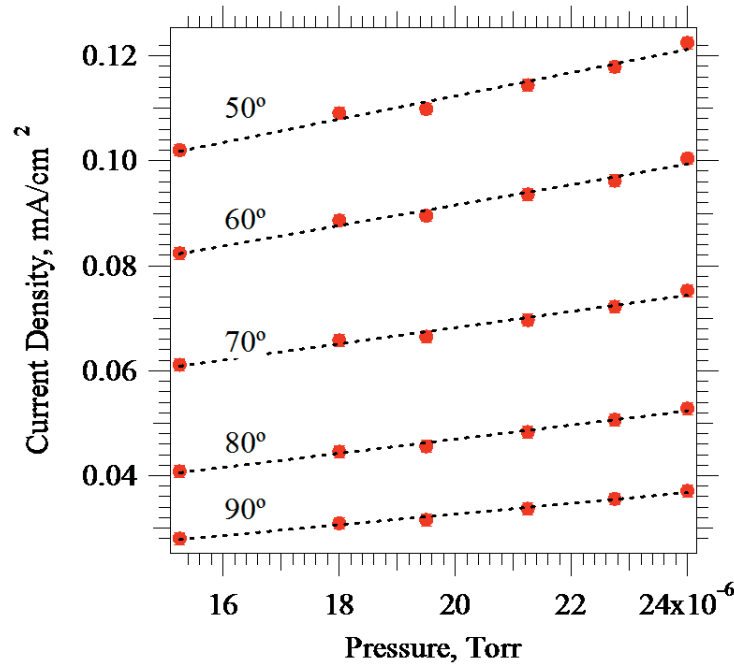
Figure 3. Linear relationship between current density in the wings and facility pressure. Linear relationship holds at other angles, not shown for clarity.

Table 2. Calculated beam current and 95% plume divergence half angle as a function of pressure, including vacuum extrapolated values.

Pressure (Torr)	Integrated Beam Current (A)	95% half angle (deg)
1.3e-5	22.5	66.5
1.5e-5	22.5	68.0
1.6e-5	22.7	68.5
1.8e-5	22.7	69.5
1.9e-5	22.9	70.0
2.0e-5	22.6	71.5
Vacuum-extrapolated	20.3	42.5

B. Performance Measurements at 6 and 8 kW

Thrust and discharge current measurements were also taken at a variety of facility pressure. Thrust measurements at the various facility pressures were taken continuously, without shutting the thruster off for zero measurements. A calibration was performed before and after the entire set of measurements and the instantaneous zero position of the thrust stand was inferred by linear interpolation.

The results for thrust and discharge current at the nominal condition of 300 V and 20 mg/s are shown in Figure 5. The linear relationship of those measurements was used to extrapolate measured results to vacuum conditions as shown in Table 3. The same procedure was used for 8-kW thruster operation at 400 V and 20 mg/s. Results are shown in Figure 6 and Table 4.

Table 3. Comparison of measured thrust, discharge current and efficiency with vacuum-extrapolated values at 300 V, 20 mg/s.

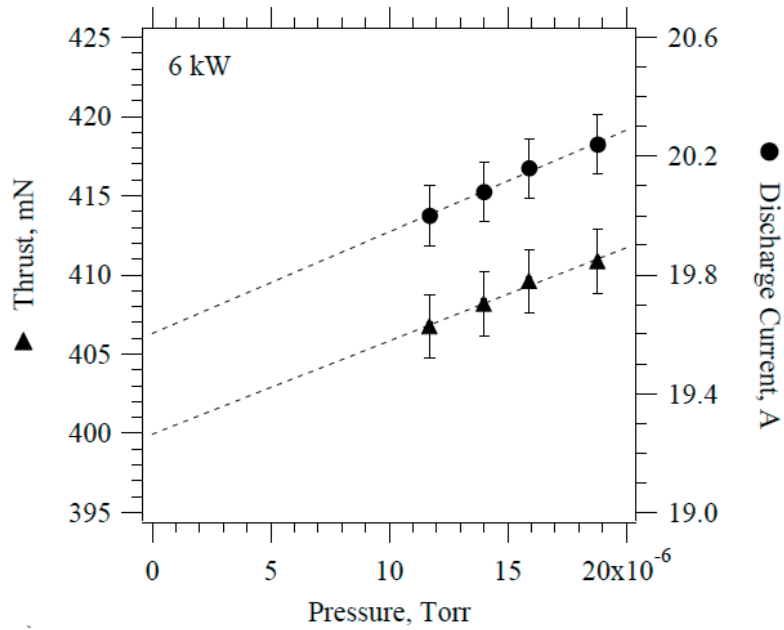|	Thrust (mN)	Discharge Current (A)	Efficiency
P = 1.9x10^{-5}	409	20.3	0.64
Vacuum	400	19.6	0.61
Change	- 2.2%	- 3.4%	-0.03 (abs)

Figure 4. Measured thrust and discharge current at 300 V, 20 mg/s with changing facility pressure, including vacuum extrapolation.

Table 4. Comparison of measured thrust, discharge current and efficiency with vacuum-extrapolated values at 400 V, 20 mg/s.

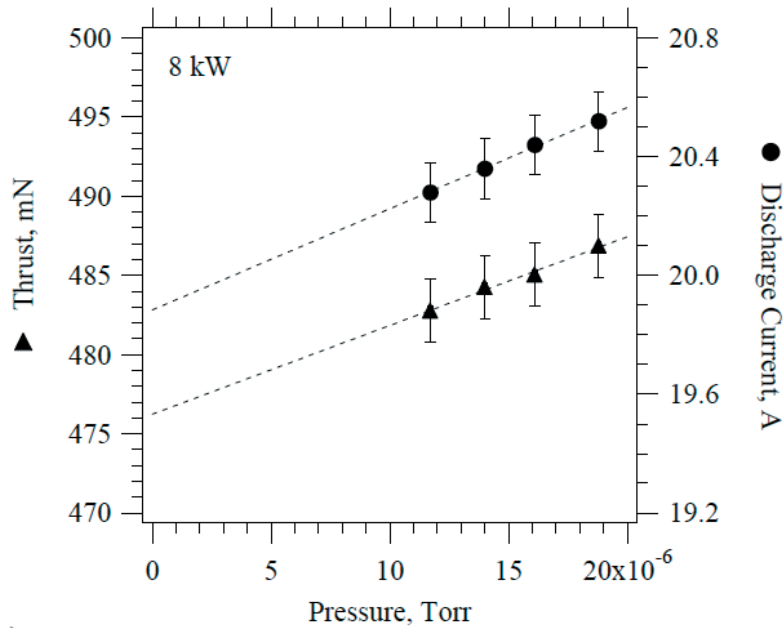|	Thrust (mN)	Discharge Current (A)	Efficiency
P = 1.9x10^{-5}	486	20.6	0.67
Vacuum	476	19.9	0.64
Change	-2.1%	-3.4%	-0.03 (abs)

Figure 5. Measured thrust and discharge current at 400 V, 20 mg/s with changing facility pressure, including vacuum extrapolation.

C. Analytical Method to Quantify Facility Effects on Performance Measurements

An augmented calculation of the entrained flow was necessary to account for the discrepancy between the predicted entrained flow and the measured increment in discharge current and thrust. Walker[19] made a similar attempt to rectify the discrepancy in measured and predicted entrained flow by considering the increment in current as a function of facility pressure. In the present treatment, the discharge current and thrust were corrected to their vacuum values by removing the contribution from facility neutrals by introducing a hemispherical entrainment area with a radius equivalent to the discharge channel outer radius. Correcting with this entrainment definition produced good agreement with experimental data that was extrapolated to zero background pressure.

1. Entrained Neutral Gas (area selection)

To evaluate the effect that higher facility pressure had on thruster performance, the effect of entrained flow due to facility neutral gas needed to be quantified. Using a derivation similar to Ref. 17, the entrained mass flow, $\dot{m}_{en}$ was calculated by integrating the random thermal mass flux of facility neutrals across a surface (usually the discharge channel exit plane) using the kinetic approximation

$$\dot{m}_{en} = A_{en} \frac{n_n m_{xe}}{4} \left(\frac{8k_B T}{\pi m_{xe}} \right)^{1/2} = A_{en} P \left(\frac{m_{xe}}{2\pi k_B T} \right)^{1/2} , \tag{1}$$

where A_{en} is the area over which the entrainment occurs, T is the temperature of the facility neutrals (assumed to be 300 K here), and P is the facility pressure. The entrained mass flow was converted to entrained discharge current by

$$I_{en} = \dot{m}_{en} \frac{e}{m_{xe}} , \tag{2}$$

where the neutrals were assumed to be singly ionized. For the simple model in Eq. 1, the entrained mass flow was primarily dependent on the facility pressure and selection of entrainment area. The uncertainty in the facility pressure reading was approximately ± 20% and the facility pressure reading was assumed to be representative of the neutral density near the thruster due to facility neutrals.

It was reasonable to assume that the entrained mass flow should be integrated over a larger area than the discharge channel cross section since the electron temperature in the first few centimeters downstream of the channel exit plane remained high enough to ionize neutral gas.[20, 21] A natural selection of area was a hemisphere at the outer diameter of the thruster channel. This boundary accounted for the regions of high electron temperature that extended beyond the confines of the discharge channel and increased the entrainment area by an order of magnitude. The hemispherical entrainment area was used to correct discharge current and thrust measurements to their vacuum values in the following sections.

2. Discharge Current Correction

Equations 1 and 2 indicate a linear relationship between discharge current due to entrained flow and facility pressure. This is consistent with the measured linear relationship of discharge current with pressure as shown in Figure 5 and Figure 6. The vacuum-corrected discharge current, I_{corr}, was calculated by subtracting the entrained current from the measured discharge current using

$$I_{corr} = I_D - I_{en} . \tag{3}$$

When the correction is performed using the discharge channel exit as the entrainment area, the discharge current correction is only 0.03 A, nearly an order of magnitude lower than the 0.24 A change measured at both 6 and 8 kW. Conversely, the corrected discharge current using a hemispherical area closely matches the vacuum extrapolated values as shown in Table 5.

Table 5. Comparison of analytically corrected and vacuum-extrapolated discharge current

Discharge Voltage	Corrected Discharge Current (A)	Vacuum extrapolated Discharge Current (A)
300 V	19.6	19.6
400 V	19.9	19.9

3. Thrust Correction

In a similar fashion to the discharge current correction, the thrust measurements can be corrected to remove the contribution from entrained mass flow by using

$$\tau_{corr} = \tau \left(1 - \zeta_{en} \frac{\dot{m}_{en}}{\dot{m}_a + \dot{m}_{en}}\right), \tag{4}$$

where τ_{corr} is the vacuum corrected thrust, τ is the measured thrust, and ζ_{en} is the entrainment utilization. ζ_{en} was introduced to account for the practical implication that not all ionized neutrals contribute to useful thrust (large divergence or ions that did not achieve full acceleration since they were produced outside the channel, beyond the primary acceleration region). When ζ_{en} is unity, the contribution from all of the entrained flow that contributed to discharge current is removed from the measured thrust. When ζ_{en} is zero, the thrust is uncorrected.

Beginning with $\zeta_{en} = 1$, the corrected thrust varied with facility pressure from 394 to 396 mN at 6 kW, and 466 to 470 mN at 8 kW (both approximately 2% below the vacuum extrapolated thrust) as shown in Table 6. The variation in corrected thrust with pressure indicates that $\zeta_{en} = 1$ was not properly chosen to account for entrainment. Once ζ_{en} is properly chosen, the thrust values are consistent across all measurements and closely match the vacuum extrapolated values from the previous section.

Table 6. Comparison of analytically corrected and vacuum-extrapolated thrust

Discharge Voltage	ζ_{en}	Corrected Thrust (mN)	Vacuum extrapolated thrust (mN)
300 V	1	394-396	400
	0.6	400.0 ± 0.4	
400 V	1	466-470	476
	0.5	476.1 ± 0.2	

These results suggest that approximately 50-60% of ingested neutrals that were ionized and contributed to higher discharge current did not contribute to useful thrust. This result was consistent with the suggestion that many of the ingested facility neutrals were ionized outside the thruster and experienced little axial acceleration. This provides additional support for the larger hemispherical entrainment area definition. The implication that many ions are created in the near-field and are potentially highly divergent may provide insight into the observed increase in current density in the wings as flow rate and pressure are increased.

4. Pressure Correction

To obtain reliable performance measurements, the facility pressure should be kept below a threshold that maintains the fraction of entrained mass flow below 3% of the anode mass flow. This threshold ensures that the uncertainty introduced by facility effects is within the uncertainty of the performance measurement, which was primarily due to mass flow rate measurement uncertainty. To calculate the maximum acceptable facility pressure, Eq. 1 can be rearranged into

$$P = \left(\frac{\dot{m}_{en}}{\dot{m}_a}\right) \frac{\dot{m}_a}{A_{en}} \left(\frac{2\pi k_B T}{m_{xe}}\right)^{1/2}, \tag{5}$$

where $\dot{m}_{en}/\dot{m}_a$ is the entrainment fraction. It is apparent from Eq. 5 that the maximum acceptable facility pressure to maintain the fraction of entrained mass flow below 3% (i.e., for $\dot{m}_{en}/\dot{m}_a < 0.03$) increases with increased anode mass flow rate. Using Eq. 5, the facility pressure should not exceed the values shown in Table 7.

Table 7. Maximum recommended facility pressure for given anode mass flow rates.

Anode mass flow rate (mg/s)	Facility Pressure (torr)
5	3.3×10^{-6}
10	6.5×10^{-6}
20	1.3×10^{-5}
40	2.6×10^{-5}

IV. Conclusion

Thrust, discharge current, and current density in the far-field were measured at various facility pressured to allow linear extrapolation of these results to their theoretical vacuum values. This method indicated that the nominal facility pressure can contribute as much at 3% (absolute) to the measured thruster efficiency. Analytical means for accounting for this effect required a new, hemispherical definition for the entrainment area. Although other mechanisms may contribute in the near-field plume, the hemispherical definition provided good results at 6 and 8 kW operating conditions. Further analytical investigation indicated that 50-60% of the neutrals ingested under this assumption contribute to elevated discharge current but not measured thrust. This suggestion may provide insight into mechanisms that increase the current density in the wings as facility pressure is increased.

Acknowledgments

References

1 Walker, M. L. R., Victor, A. L., Hofer, R. R. and Gallimore, A. D., "Effect of Backpressure on Ion Current Density Measurements in Hall Thruster Plumes," Journal of Propulsion and Power, 21, 3, 408-415, 2005.

2 Azziz, Y., Martinez-Sanchez, M. and Szabo, J., "Determination of in-Orbit Plume Characteristics from Laboratory Measurements," *42nd AIAA/ASME/SAE/ASEE Joint Propulsion Conference*, AIAA-2006-4484, Sacramento, CA, Jul. 9-12, 2006.

3 Hofer, R. R., Peterson, P. Y. and Gallimore, A. D., "Characterizing Vacuum Facility Backpressure Effects on the Performance of a Hall Thruster," *27th International Electric Propulsion Conference*, IEPC-2001-045, Pasadena, CA, Oct. 15-19, 2001

4 Manzella, D. H., "Hall Thruster Ion Beam Characterization," 31st AIAA/ASME/SAE/ASEE Joint Propulsion Conference, AIAA-1995-2927, San Diego, CA, Jul. 10-12, 1995.

5 Walker, M. L. R. and Gallimore, A. D., "Neutral Density Map of Hall Thruster Plume Expansion in a Vacuum Chamber," Review of Scientific Instruments 76, 5, 053509 (2005).

6 Walker, M. L. R., Gallimore, A. D., Boyd, I. D., and Cai, C., "Vacuum Chamber Pressure Maps of a Hall Thruster Cold-Flow Expansion," Journal of Propulsion and Power 20, 6, 1127-1131 (2004).

7 Nakles, M. R. and Hargus, W. A., "Background Pressure Effects on Ion Velocity Distribution within a Medium-Power Hall Thruster," Journal of Propulsion and Power 27, 4, 737-743 (2011).

8 Hofer, R. R., Anderson, J. R., "Finite Pressure Effects in Magnetically Shielded Hall Thrusters," 50th AIAA/ASME/SAE/ASEE Joint Propulsion Conference, Cleveland, OH, Jul. 28-30, 2014.

9 Reid, B. M., "The Influence of Neutral Flow Rate in the Operation of Hall Thrusters," Ph.D. Dissertation, Aerospace Engineering Dept., Univ. of Michigan, Ann Arbor, MI 2009.

10 Haas, J. M., Hofer, R. R., Brown, D. L., Reid, B. M. and Gallimore, A. D., "Design of the H6 Hall Thruster for High Thrust/Power Investigation," 54th JANNAF Propulsion Meeting, Denver, CO, May 14-17, 2007

11 Reid, B. M., Gallimore, A. D., Hofer, R. R., Li, Y. and Haas, J. M., "Anode Design and Verification for the H6 Hall Thruster," 54th JANNAF Propulsion Meeting, Denver, CO, May 14-17, 2007.

12 Reid, B. M., Gallimore, A. D., Hofer, R. R., Li, Y. and Haas, J. M., "Anode Design and Verification for a 6-kW Hall Thruster," JANNAF Journal, 2008.

13 Brown, D. L., Reid, B. M., Gallimore, A. D., Hofer, R. R., Haas, J. M., et al., "Performance Characterization and Design Verification of the H6 Laboratory Model Hall Thruster," 54th JANNAF Propulsion Meeting, Denver, CO, May 14-17, 2007.

14 Hofer, R. R., Goebel, D. M. and Watkins, R. M., "Compact LaB6 Hollow Cathode for the H6 Hall Thruster," 54th JANNAF Propulsion Meeting, Denver, CO, May 14-17, 2007.

15 Haag, T. W., "Design of a Thrust Stand for High Power Electric Propulsion Devices," 25th AIAA/ASME/SAE/ASEE Joint Propulsion Conference, AIAA-1989-2829, Monterey, CA, Jul. 10-13, 1989.

16 Walker, M., Hofer, R.R., and Gallimore, A. D., "The effects of nude Faraday probe design and vacuum facility backpressure on the measured ion current density profile of Hall thruster plumes." Joint Propulsion Conference, AIAA-02-4253, Indianapolis, Indiana. 2002.

17 Randolph, T., Kim, V., Kaufman, H. R., Kozubsky, K., Zhurin, V. V., et al., "Facility Effects on Stationary Plasma Thruster Testing," 23rd International Electric Propulsion Conference, Seattle, WA, Sept. 13-16, 1993.

18 Boyd, I. D., "Review of Hall Thruster Plume Modeling," Journal of Spacecraft and Rockets, 38, 3, 381-387, 2001.

19 Walker, M. L. R. and Gallimore, A. D., "Performance Characteristics of a Cluster of 5-kW Laboratory Hall Thrusters," Journal of Propulsion and Power, 23, 1, 2007.

20 Reid, B. M. and Gallimore, A. D., "Plasma Potential Measurements in the Discharge Channel of a 6-kW Hall Thruster," 44th AIAA/ASME/SAE/ASEE Joint Propulsion Conference, AIAA- 2008-5185, Hartford, CT, Jul. 20-23, 2008.

21 Reid, B. M. and Gallimore, A. D., "Langmuir Probe Measurements in the Discharge Channel of a 6-kW Hall Thruster," 44th AIAA/ASME/SAE/ASEE Joint Propulsion Conference, AIAA- 2008-4920, Hartford, CT, Jul. 20-23, 2008.